Hindawi
Adsorption Science & Technology
Volume 2022, Article ID 7138770, 13 pages
https://doi.org/10.1155/2022/7138770

Research Article

Synthesis and Characterization of New Catalysts Grains Based on Iron(Oxy)Hydroxides supported on Zirconium for the Degradation of 4-Nitrophenol in Aqueous Solution

Hafsa Loumi,[1,2] Faiza Zermane,[1,2] Benamar Cheknane,[1,2] Naima Bouchenafa,[1] Omar Bouras,[2] and Adrián Bonilla-Petriciolet[3]

[1]*Laboratoire Chimie Physique Des Interfaces Des Matériaux Appliqués à l'Environnement, Département de Génie Des Procédés, Université Saad Dahlab Blida 1, 09000 Blida, Algeria*
[2]*Laboratoire Eau Environnement et Développement Durable, Département de Génie Des Procédés, Université Saad Dahlab Blida 1, 09000 Blida, Algeria*
[3]*Instituto Tecnológico de Aguascalientes, Aguascalientes 20256, Mexico*

Correspondence should be addressed to Adrián Bonilla-Petriciolet; petriciolet@hotmail.com

Received 22 December 2021; Revised 21 January 2022; Accepted 21 April 2022; Published 14 May 2022

Academic Editor: Hesham Hamad

This study reports the preparation of catalyst grains based on oxyhydroxides of iron and zirconium via the coprecipitation method and their application in the degradation of 4-nitrophenol. The morphology, microstructure, and surface composition of these catalysts were characterized by scanning electron microscopy, X-ray diffraction, nitrogen physisorption, and Fourier transform infrared spectroscopy. The catalytic activity of the grains was assessed in the degradation of 4-nitrophenol in a heterogeneous system at different operating conditions. Degradation rates up to 93% were obtained after 4 h of contact time where the catalytic activity of tested materials was higher at pH 7 than in acidic and basic conditions. Amorphous iron hydroxide with a ratio of 75% Zr+25%Fe showed the best catalytic properties. These novel materials are an interesting alternative for facing the water pollution caused by organic compounds.

1. Introduction

The environment has been impacted seriously by a variety of pollutants generated by both anthropogenic and geogenic sources [1]. In particular, the presence of organic matter from the discharge of untreated industrial wastewaters is an important source of environmental pollution. 4-Nitrophenol (4-NP) is an organic pollutant commonly found in wastewaters and contaminated soils [2]. It is used as a chemical intermediate for the preparation of insecticides (e.g., methyl parathion), the production of azo and sulfur dyes, rubber chemicals, lumber preservatives, and other industrial applications [3]. This phenolic compound is considered toxic and harmful for human health [4]. Literature indicates that the chronic exposure to this and other phenolic compounds can be associated to several health problems such as impairment of pancreas, liver and kidney and can also cause the paralysis of the central nervous system [5, 6]. The Environmental Protection Agency of United States (US-EPA) has classified 4-NP in the first category of dangerous products that pollutes the environment through the improper disposal of industrial and agricultural wastewaters thus affecting the soils and water sources and generating the conditions for its accumulation in the food chain [7].

Phenolic compounds in wastewaters can be removed by various physical and chemical techniques [8, 9]. Therefore, the complete degradation and/or mineralization of these chemicals via effective and low-cost processes is a challenging task [10–14]. The treatment of water polluted by organic compounds via oxidation processes is an effective and low cost solution. These oxidation processes utilize catalyst to improve the degradation performance [15]. In particular,

heterogeneous catalysts can be employed in the removal of organic compounds. These materials not only preserve the activity and selectivity offered by homogeneous catalysts but also allow their facile recovery and reuse in subsequent oxidation processes [15].

Several studies showed that a variety of heterogeneous catalysts can be utilized for the degradation of organic compounds in wastewater treatment. Zirconia and Fe-supported zirconia have been used as heterogeneous catalysts in photocatalytic advanced oxidation processes [16–20]. For instance, the wet oxidation of phenol via heterogeneous catalysis using materials based on iron and copper and hydrogen peroxide was carried out under normal conditions of temperature and pressure [21]. Results of this study showed a great stability of tested catalysts in the aqueous medium. Saeed and Ilyas [6] demonstrated that the nickel hydroxide was more effective to degrade phenolic compounds. The application of iron-based catalysts (e.g., Fe-TiO_2 and Fe-C-TiO_2) played an important role to accelerate the oxidation rate of phenol [6]. Espinosa et al. [22] studied the wet oxidation of phenol on metallic catalysts (Ru, Pt) supported on TiO_2-CeO_2 and showed that platinum-based catalysts were more effective than those based on ruthenium. Idrissi et al. [23] used a manganese-based catalyst supported on a bentonite for the oxidation reaction of phenol in a diluted aqueous solution. Catalytic tests showed that the solids based on Mn at 5% were more active but they were unstable in the aqueous solution compared to bentonite alone. However, the reduction in total organic carbon remained low for all the studied catalysts. The degradation of 4-NP was also analyzed by Gaffour and Mokhtari [2] using the advanced oxidation processes at room temperature where the mineralization of this compound was effective. On the other hand, the Fenton process showed that the degradation and reduction rates increased with the catalyst ratio and treatment time where the best oxidation process used UV/H_2O_2/Fe^{2+} [2]. Sable et al. [4] synthesized heterogeneous catalysts from 4% Fe impregnated with ZrO_2, which were used in the Fenton-like process for the phenol degradation. Othman et al. [24] demonstrated the catalytic activity of copper and nickel in an aqueous medium. These metallic species were very effective in the oxidation reaction of phenol. Results also showed that phosphate coated $CuFe_2O_4$ were competitive Fenton-type catalysts for phenol degradation [24]. Although significant advances have been achieved in the preparation of photocatalysts for the degradation of organic compounds, there are still several challenges to be resolved with the aim of reducing the operational costs of this treatment technology for large-scale applications. Herein, it is convenient to remark that different synthesis procedures can be utilized and optimized to tailor the properties of catalytic materials including the application of biopolymers to obtain composites with improved properties for the removal of organic pollutants [25–27]. For instance, various nanocomposites of TiO2–ZnO, TiO2–ZnO/CS, and TiO2–ZnO/CS–Gr were synthesized by Patehkhor et al. [28] using sol–gel and ultrasound-assisted methods. These materials were utilized to enhance the photocatalytic degradation of tetracycline under UV irradiation where the best material showed 97% of efficiency in the degradation of tetracycline after 3 h. On the other hand, it is also important to analyze the kinetic and thermodynamic parameters related to the removal of organic pollutants using catalytic materials [25].

Considering this background, the main objective of this study was to synthesize catalysts in the form of grains based on a mixture of iron(oxy)hydroxides, especially amorphous iron hydroxide (HFO) and goethite, and zirconium for the catalytic oxidation of 4-NP under the presence of hydrogen peroxide. Degradation tests are reported in this paper including the physicochemical characterization of tested catalyst. The novelty of this study relied on the preparation of hybrid catalytic materials using iron (oxy)hydroxides supported by zirconium where their powders were shaped into grains of different sizes using the wet granulation method. Results reported in this study showed that this catalyst was effective for the 4-NP degradation from aqueous solution.

2. Materials and Methods

2.1. Preparation of Catalysts. Two (oxy)hydroxides iron solids (i.e., goethite and HFO) were used in this study. The catalysts were obtained via the coprecipitation method with different Fe/Zr ratios. Specifically, these materials were prepared following the next protocol. First, the synthesis of HFO was carried out according to the method reported by Jiang et al. [29]. This protocol consisted of dissolving slowly, with stirring and bubbling N_2, 60 g of NaOH pellets in 500 mL of a solution of $Fe(NO_3)_3.9H_2O$ (0.5 M) (>98%, Prolabo) and $ZrO(NO_3)_2.H_2O$ (>99%). This mixture reacted to form a solid product. After removing the supernatant, the solid was separated by centrifugation, washed twice with double-distilled water, and dried in an oven at 25°C. After grinding, the powder (goethite-Zr) was recovered in a dark bottle and protected against possible pollution by organic products.

The preparation of goethite-based catalyst was performed as follows. Goethite, α-FeO(OH), was synthesized according to the protocol of Wu et al. [30]. It implied the rapid mixing of 100 mL of $Fe(NO_3)_3.9H_2O$ (1 M) (>98%, Prolabo) and $ZrO(NO_3)_2.H_2O$ (>99%) with 180 mL of NaOH (5 M) (>98%, Prolabo) under stirring and bubbling N_2 to avoid carbonation with atmospheric CO_2. The mixture was then diluted to 2 L with double-distilled water and placed in an oven at 70°C for 60 h. The final precipitate was washed several times with 500 mL of double-distilled water to remove the excess of nitrates. After drying at 60°C for 24 h, the solid was grounded until a homogeneous powder was obtained and the final product was stored in a dark bottle.

HFO-Zr and goethite-Zr catalysts with different compositions were prepared where Table 1 provides the sample labels and their characteristics. On the other hand, the preparation of uniform catalyst grains was carried out using a granulator with a high shear rate, see Figure 1. Table 2 provides the operating conditions of the granulation process, which were optimized by Cheknane [31]. First, 20 g of powder catalyst were introduced into the high shear mixer with a

rotation speed of 600 rpm to homogenize at the dry state. This step was followed by wet granulation that consisted of spraying the binder solution (industrial grade silicone) on the powder bed by varying the mixer speed from 100 to 1000 rpm for 6 min. At the end of granulation, the grains were collected carefully and placed on a plate and dried in a tray oven at 60°C. This temperature was chosen to allow the evaporation of wetting agent (water), while the main characteristics of the binding agent (industrial grade silicone) and catalyst were retained [29]. The final product was then calcined at 500°C for 3 h with a heating rate of 5°C/min.

2.2. Physicochemical Characterization of Catalysts. Different characterization techniques were used to analyze the morphology and surface properties of catalysts where the results were used to explain their performance and selectivity. In particular, XRD analysis was carried out with a X-ray diffractometer (Model Rigaku) with scanning rate of 5°/min from 5° to 80°, ceramic tube with copper and generator power at RX: 40 mA, 40 kV. XRD results were obtained with an angular step of 0.05° at 2 s per step and sample rotation with 0.02°. These results were utilized to identify the crystalline phases and the presence of (oxy)hydroxides. Fourier transform infrared spectroscopy (Perkin-Elmer FTIR spectrometer 310) was used to analyze the functional groups present on the catalyst surface. FTIR spectra were recorded at 400-4000 cm^{-1} with resolution of 2 cm^{-1}. The measurements were made via diffuse reflection. Catalyst samples were analyzed in the form of fine pellets using KBr. BET areas of tested samples were measured by a model Quantachrome NOVA WIN 2 automated gas sorption system. Surface morphology of samples were analyzed with a scanning electron microscopy (SEM) Quanta 650 (FEI). The pH of point of zero charge (PZC) was determined for catalyst samples. First, 0.03 g of catalyst were added to 30 mL Erlenmeyer flasks containing a solution of potassium nitrate (0.1 M) adjusted to different pH values (from 2 to 12). The initial pH of solution (pHi) was adjusted by 0.1 M KOH and 0.1 M HNO_3. This solution was stirred at 225 rpm for 24 h at 24°C, and the final pH of supernatant liquid (pHf) was measured after filtration with a 0.45 μm filter paper. PZC was associated to the value of initial pH when the ΔpH equals to zero.

Finally, some mechanical properties of the catalyst grains were also analyzed. First, the friability is a property that describes the mechanical resistance of grains subjected to impact and/or abrasion. Therefore, the friability measurements of catalyst samples were carried out by introducing 1 g of sample ($P1$) in a friabilimeter (Roche ERWEKA TA3R, Germany) for 10 min at a speed of 25 rpm. After a rotation of 250 turns, the grains were weighed (P2), and the friability index (F%) was calculated with the following equation:

$$F(\%) = \frac{P1 - P2}{P1}.100. \quad (1)$$

The settlement of powders reflects the ability of particles to rearrange spontaneously (under the effect of gravity) and then under the effect of mechanical stresses (under the effect of successive falls). Therefore, the test described in the European Pharmacopoeia was used to study the behavior of powders, placed in a test tube, and subjected to successive and standardized falls. In a 250 mL graduated cylinder, a sufficient amount of grain, not more than 100 g, was introduced without packing and the apparent volume (V_0) was recorded. Then, the sample was submitted to 50 and 100 strokes and the apparent volumes corresponding to V_{50moy} and V_{100moy} were also recorded. The compaction capacity (V) was calculated as follows:

$$V = V50 - V100. \quad (2)$$

The settling ability was associated to the Carr index (IC) by the following expressions:

$$\mathrm{IC} = \frac{V50 - V100}{V50}.100 = \frac{\text{settlement}}{V5O}.100. \quad (3)$$

Catalytic studies for the degradation of 4-nitrophenol.

The activity of catalysts was tested in the oxidation reaction of 4-NP under the presence of H_2O_2. 4-NP oxidation reaction was performed in a discontinuous system using 0.2 g of catalyst, 200 mL of 11 mg/L solution of 4-NP and 10 mL of hydrogen peroxide. This 4-NP concentration was selected considering that some discharges in Algeria showed concentrations lower than 20 mg/L. Degradation experiments were performed under the bubbling of N_2 and proper agitation at room temperature. Liquid samples were taken regularly in order to follow the evolution of 4-NP oxidation. The oxidation products were analyzed by high-performance liquid chromatography (HPLC) with a C18 column.

The conversion of 4-NP during the catalytic degradation was estimated and calculated using the next equation:

$$\text{Conversion} = 100\left(1 - \frac{Cr}{C0}\right), \quad (4)$$

where $C0$ and Cr are the initial and final concentrations of 4-NP in the corresponding degradation study.

Table 1: Composition of catalysts prepared for the degradation of 4-nitrophenol in water.

Catalyst composition	Precursor	Sample
75%Fe + 25%Zr	Goethite	75GFe25Zr
50%Fe + 50%Zr	Goethite	50GFe50Zr
25%Fe + 75%Zr	Goethite	25GFe75Zr
75%Fe + 25%Zr	HFO	75HFe25Zr
50%Fe + 50%Zr	HFO	50HFe50Zr
25%Fe + 75%Zr	HFO	25HFe75Zr

3. Results and Discussion

3.1. Characterization of Catalysts. X-ray diffraction patterns of analyzed samples are given in Figure 2. They showed

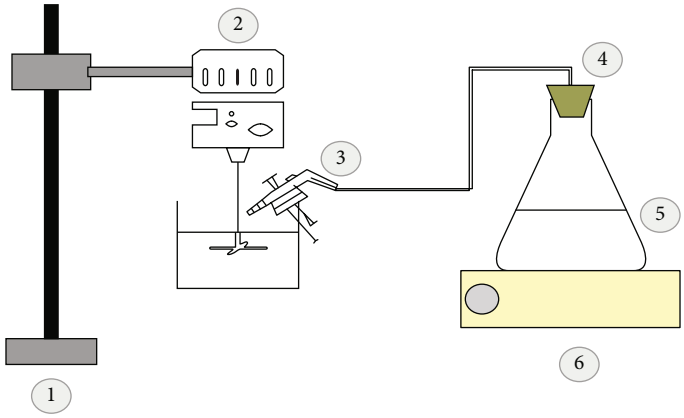

Figure 1: Configuration of mixer granulator used in the preparation of catalyst for the degradation of 4-nitrophenol. (1) Support, (2) mechanical stirrer, (3) sprayer, (4) plug, (5) Erlenmeyer flask, and (6) magnetic stirrer.

Table 2: Operating conditions used in the granulation process of catalyst.

Mass of the powder, g	20
Rotation speed of the studied mixer, rpm	100 to 1000
Concentration of the binder solution, %	40
Duration of the process, min	6

peaks located at $2\theta \geq 20^{\circ}$ attributed to the different iron (oxy)hydroxides. These iron species were present with percentages varying from 8 to 11% mainly for α-FeOOH and HFO. Note that these findings agreed with results reported by other authors [32]. All XRD patterns exhibited two peaks at 2θ ranges of 15°-40° and 40°-70°, thus indicating the amorphous nature of solids [33]. It was found that zirconia existed mainly in the monoclinic phase and only a very small peak was associated to the tetragonal phase according to JCPDS No. 42-1164. XRD results also showed the disappearance of the peaks in the diffraction pattern of HFO and α-FeOOH-based materials that were initially present in the raw feedstock, and it was also identified the intensification of certain peaks located at $2\theta = 22$, 34, and 37° related to goethite. XRD pattern of the former catalyst showed peaks at $2\theta = 28.5$ and 31.8, thus indicating the retention of monoclinic phase of zirconium. However, the monoclinic phase of zirconia was lost in the catalyst, which was probably due to the presence of water. Debye-Scherrer equation was utilized to estimate the size of iron oxide aggregates, which ranged from 25 to 34 nm.

FTIR spectra of tested catalysts are reported in Figure 3. The coexistence between zirconium and ferric (oxy)hydroxides was associated to the intense absorption bands at 4000-3500 cm^{-1} as well as those located at 1500 cm^{-1} that were characteristic of (oxy) iron hydroxides, i.e., the bands located at 4000 and 3630 cm^{-1} (wide) and 1630 up to 1480 cm^{-1} (small). The (oxy)hydroxides were related to the absorption band at 1635 cm^{-1} that was attributed to the deformation vibrations of H_2O molecules. The band located at 3625 cm^{-1} of the goethite spectrum corresponded to the vibration of OH bond. The absorption bands identified at 3320 and 1640 cm^{-1} were assigned to the asymmetric stretching and bending modes of OH groups while the weak absorption band at 837 cm^{-1} was attributed to Zr-O stretching mode.

BET surface areas of all the materials are reported in Table 3. Overall, the HFO-based catalysts showed higher specific surface areas than goethite. Note that this textural parameter partially explained the results of oxidation reaction for the catalysts prepared with HFO and zirconium. For illustration, Figure 4 shows the N_2 adsorption-desorption isotherm at 77 K of the catalyst 25HFe75Zr. This isotherm can be considered as type IV according to the IUPAC classification, which is characterized of a monolayer adsorption with the presence of mesopores. Calculated BET surface area of this sample was 267.66 m^2/g with a pore volume of 0.262 cm^3/g.

SEM images were used to examine the morphology of supports, the presence of grains, and porosity in the goethite and HFO-based catalysts. SEM images of goethite and HFO showed rather opaque and nonregular structures, thus reflecting the existence of these (oxy)hydroxides in the form of a precipitate, see Figure 5(a). Catalyst samples with different compositions also presented a regular and orderly morphology where spherical-like forms were observed. The results of elemental analysis of tested samples confirmed the presence of iron, zirconium, and some traces of silica and aluminum, see Figure 5(b).

Table 4 reports the PZC values for different materials studied, which ranged from 4.1 to 10.42 in powder form and from 6.07 to 11.12 in grain form. As stated, PZC corresponds to the pH value where the net surface charge of a solid surface is zero. Surface charge of solids can be positive, negative, or zero depending on the solution pH. At pH < PZC, the surface charge of the material is positive and otherwise is negative if pH > PZC. Therefore, this property contributes to understand the phenomena that can occur during the catalytic process and helps to interpret the influence of solution pH on the pollutant degradation. Finally, Table 5 shows the results for the mechanical tests performed on the grains. The compaction capacity of all the grains ranged from 5 to 17 mL, which was consistent with standard

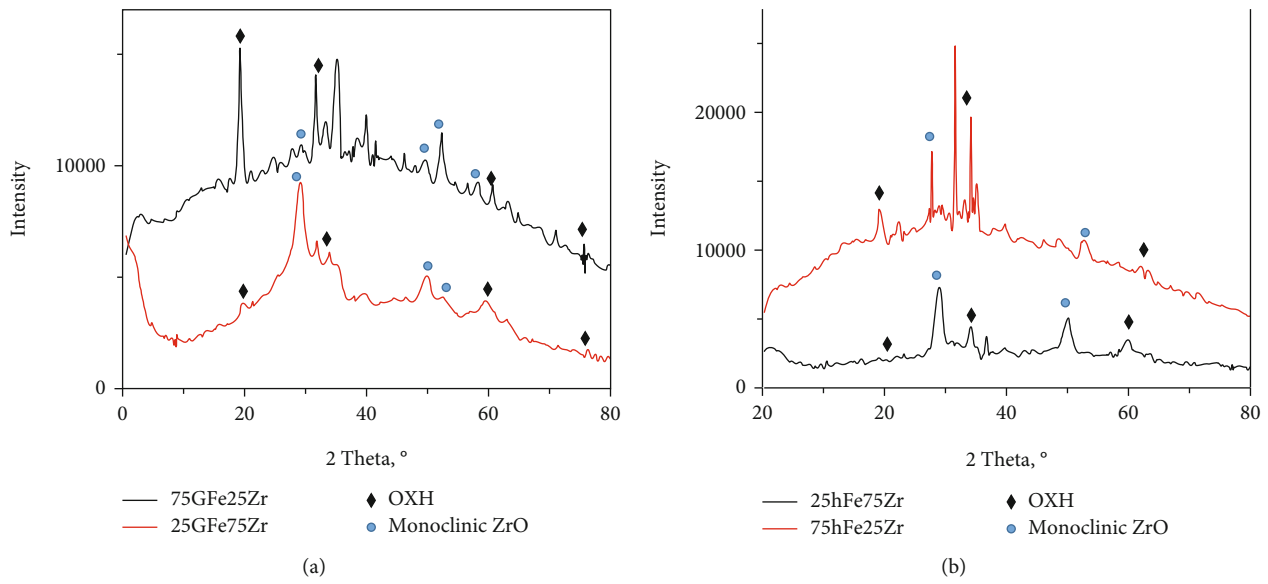

Figure 2: X-ray diffraction patterns of catalyst samples used in the degradation of 4-nitrophenol.

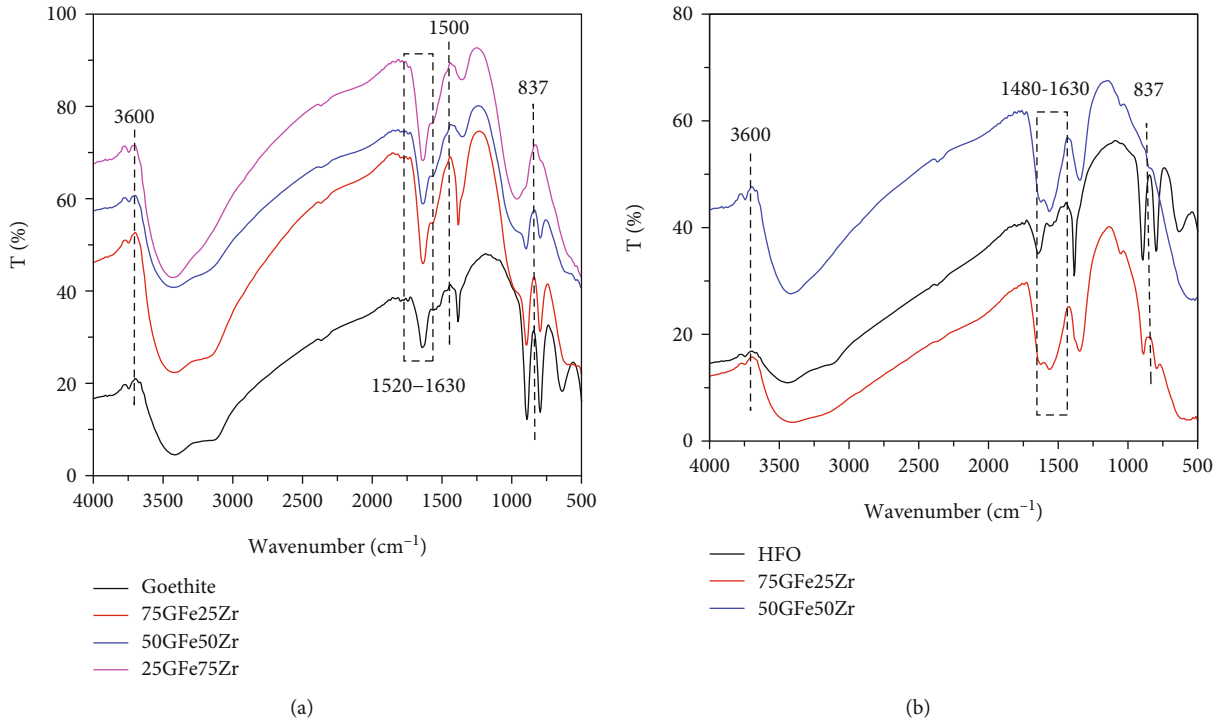

Figure 3: FTIR spectra of catalyst samples used in the degradation of 4-nitrophenol.

Table 3: Main textural parameters of catalysts prepared in this study.

Sample	BET surface area, m^2/g	Pore volume, cc/g
75HFe25Zr	213.911	0.159
50HFe50Zr	236.418	0.2567
25HFe75Zr	267.661	0.261
50GFe50Zr	232.551	0.1682
75GFe25Zr	114.809	0.12
25GFe75Zr	188.496	0.1464

values (European pharmacy). The friability of catalyst grains was lower than 1%.

3.2. Impact of Operating Conditions on the 4-NP Degradation. The results of the effect of contact time on the conversion rate of 4-NP are given in Figure 6(a). A rapid degradation rate of 4-NP was observed at <30 minutes followed by a significant slower 4-NP degradation between 50 to 90 min. 4-NP removal rates were stabilized at

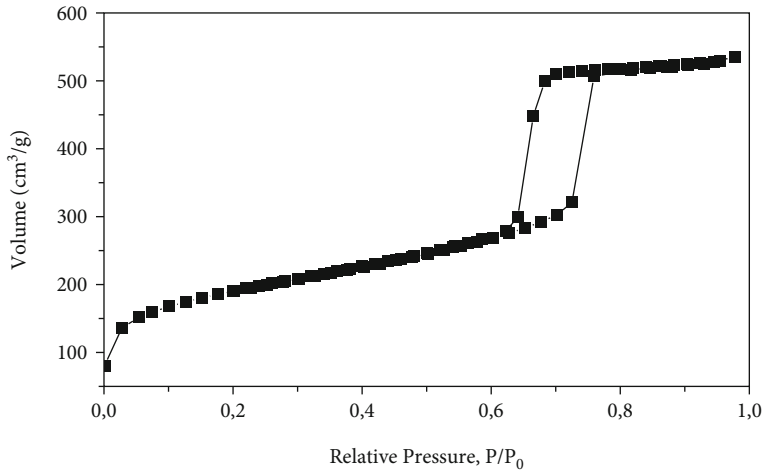

Figure 4: N_2 adsorption-desorption isotherms at 77 K of catalyst sample 25HFe75Zr.

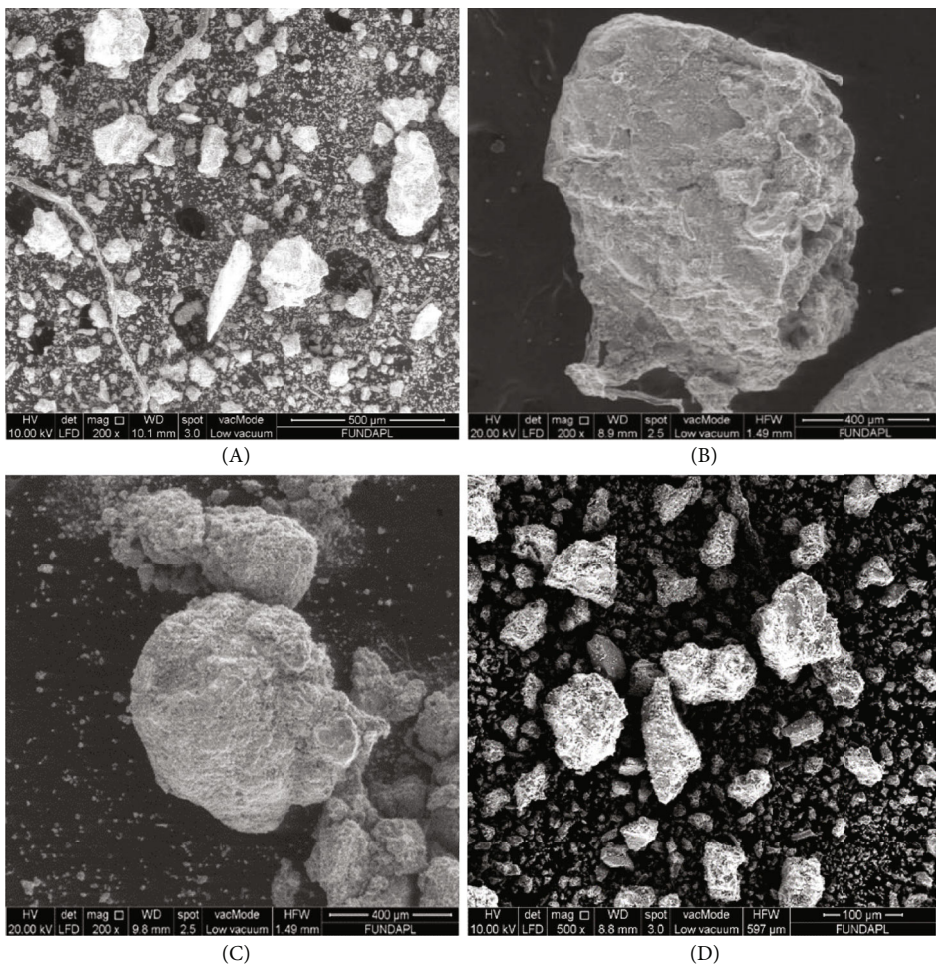

(a) SEM images

Figure 5: Continued.

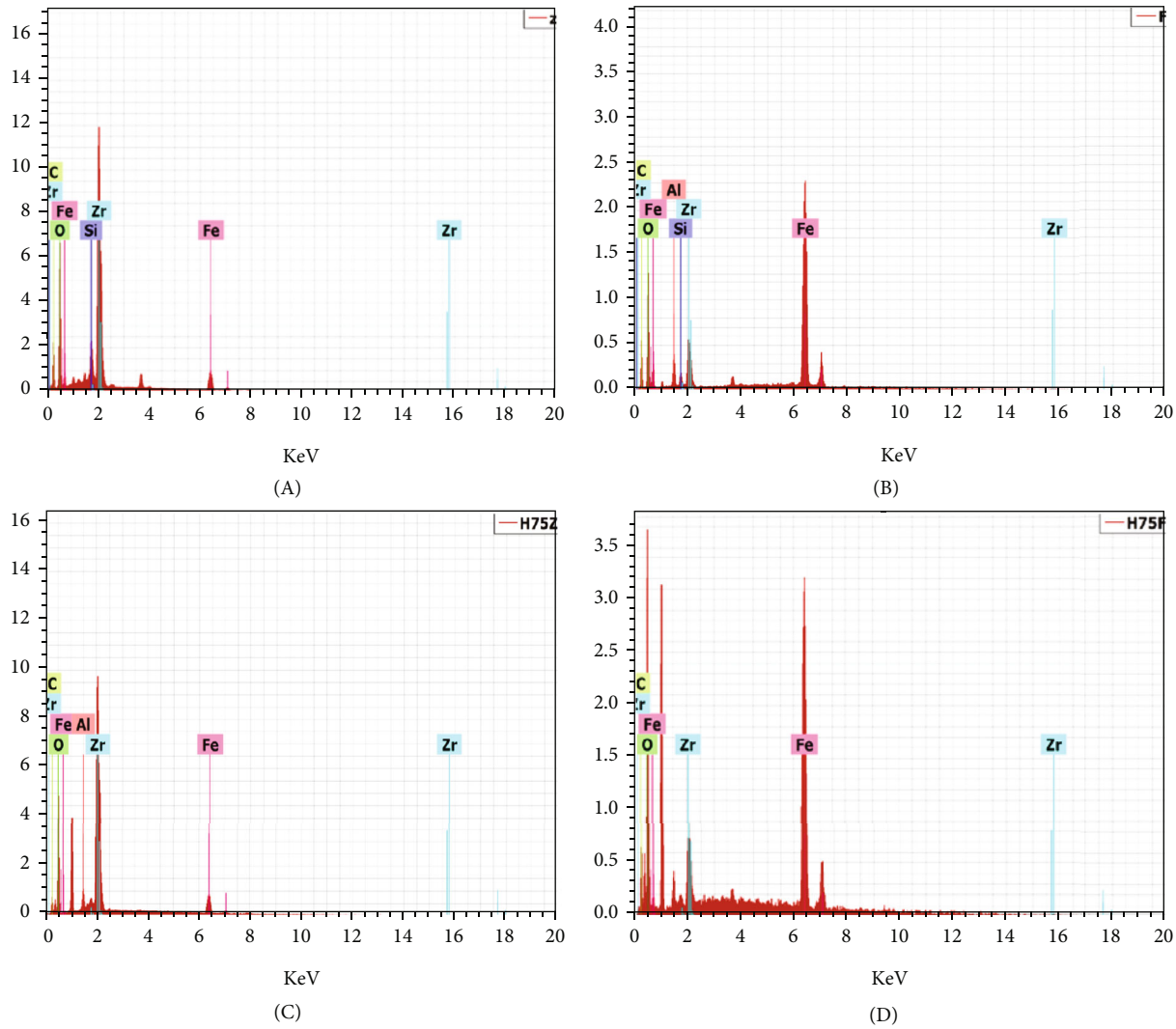

Figure 5: (a) SEM images and (b) EDX results of catalyst samples in grain form. Samples: (I) 25GFe75Zr, (II) 75GFe25Zr, (III) 25HFe75Zr, (IV) 75HFe25Zr.

Table 4: pH of point of zero charge (PZC) of catalysts used in the degradation of 4-nitrophenol.

Sample	PZC	
	Powder	Grain 0.4 mm < d < 1 mm
25GFe75Zr	7.13	9.17
75GFe25Zr	7.18	11.12
50GFe50Zr	7.01	9.40
Goethite	6.1	9.07
25HFe75Zr	4.11	6.07
75HFe25Zr	8.14	11.20
50HFe50Zr	8.19	8.67
HFO	10.42	8.31

>90 min. These degradation rates can be explained by the effect of the external diffusion associated to the concentration gradient at the beginning of the reaction.

Table 5: Mechanical properties of the catalysts used in the degradation of 4-nitrophenol.

Sample	Friability, %	Settlement, mL
HFO	0.1	5
75HFe25Zr	0.1	14.29
25HFe75Zr	0.2	11.11
Goethite	0.2	14.28
75GFe25Zr	0.1	15
25GFe75Zr	0.3	16.66
Standards	<1%	<20

Catalytic tests were also carried out with different catalyst amounts using an initial 4-NP concentration of 11 mg/L at pH 7 and 27°C, see Figure 6(b). Results showed that the best catalyst mass was 0.2 g to obtain a conversion rate of 81%. On the other hand, the effect of 4-NP concentration

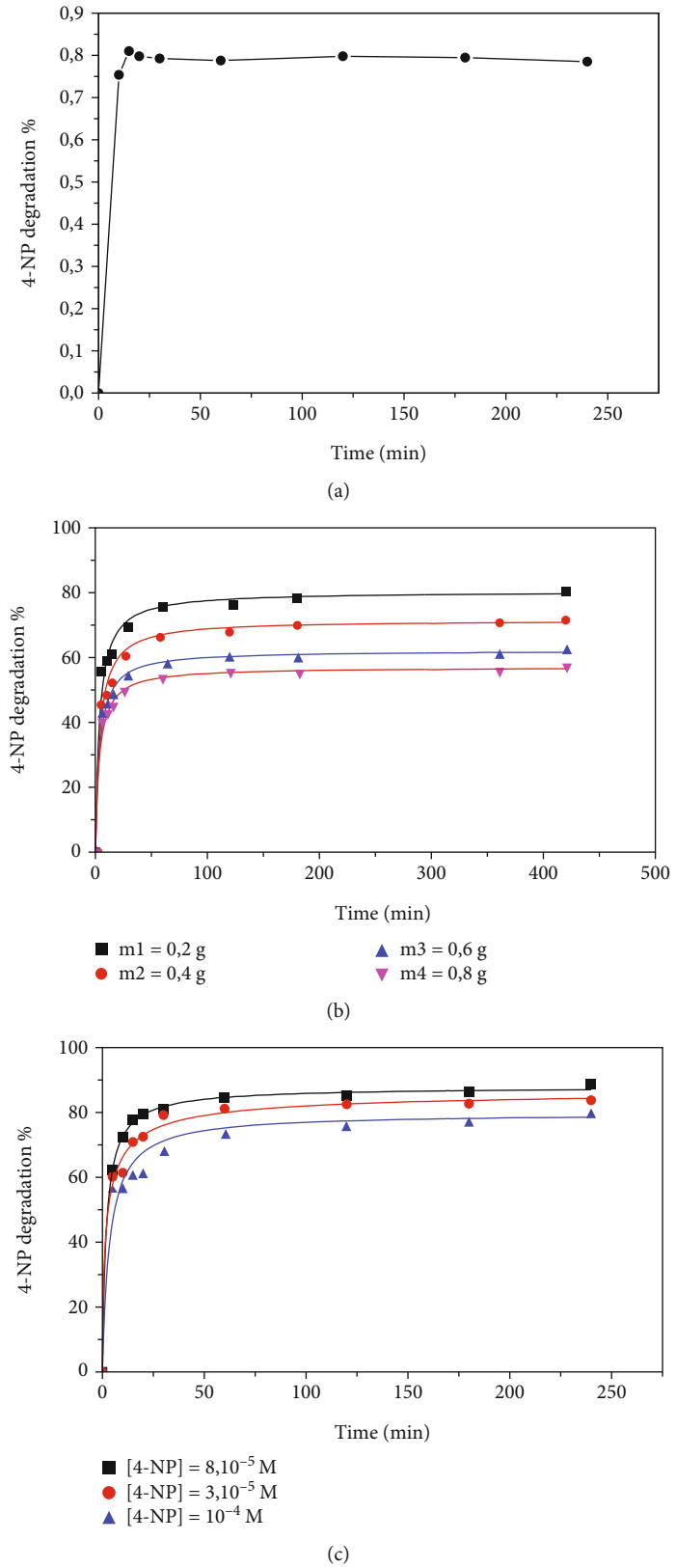

Figure 6: Effect of contact time, catalyst mass, and 4-nitrophenol concentration on the degradation yield via catalytic oxidation. Experimental conditions: (a) 0.2 g of catalyst, 11 mg/L of 4-nitrophenol concentration, pH 7, and 27°C, (b) 11 mg/L of 4-nitrophenol concentration, pH 7, and 27°C, (c) 0.2 g of catalyst, pH 7, and 27°C.

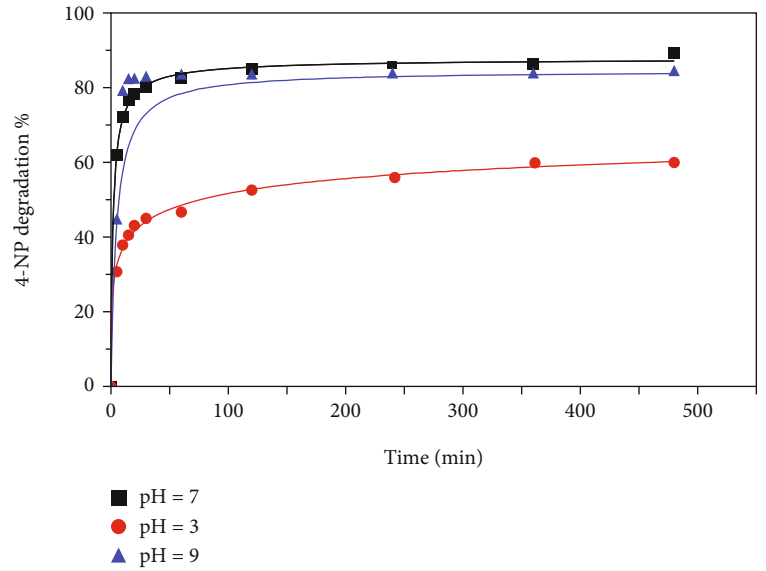

(a) 0.4 mm < d < 1 mm

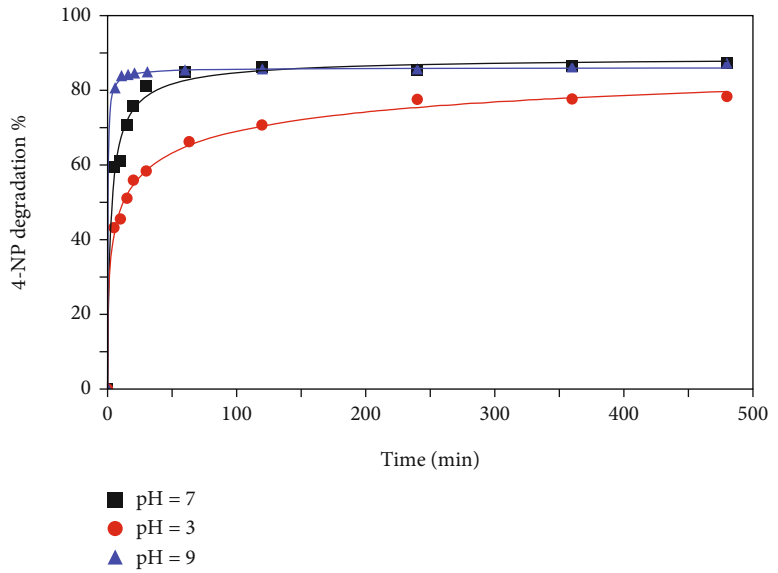

(b) 1 mm < d < 2 mm

Figure 7: Continued.

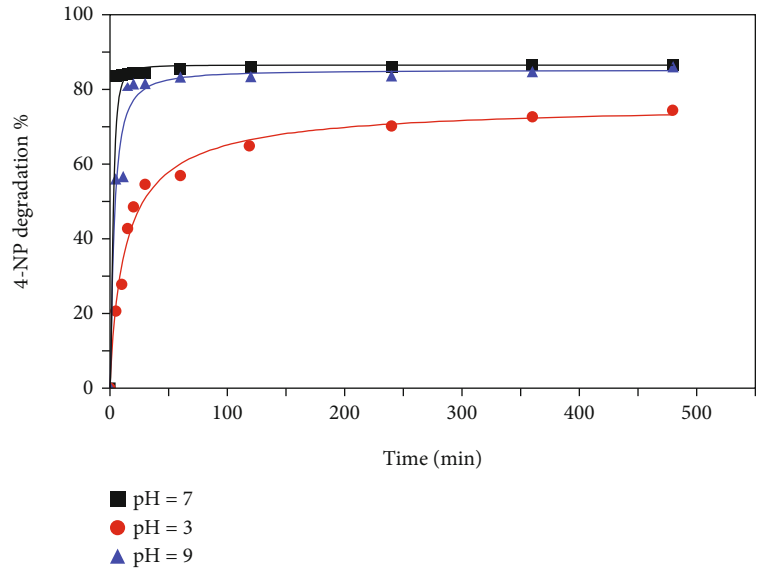

(c) 2 mm < d < 2.5 mm

Figure 7: Effect of solution pH on the 4-nitrophenol degradation by catalytic oxidation using catalyst grains with different diameters. Experimental conditions: 0.2 g of catalyst, 11 mg/L of 4-nitrophenol concentration, and 27°C.

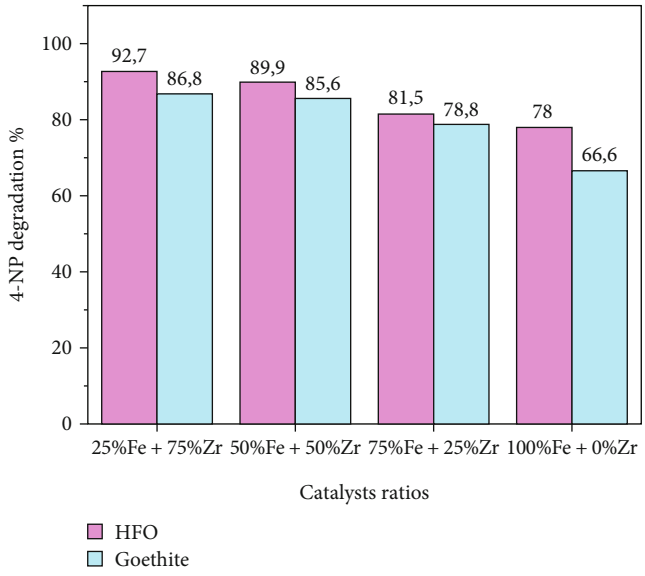

Figure 8: 4-Nitrophenol degradation efficacy of tested catalysts at pH 7, 27°C, and 4 h.

on the degradation efficiency was tested, and results are reported in Figure 6(c) for concentrations of $8{\cdot}10^{-5}$–$1{\cdot}10^{-4}$ M. An increment in the pollutant concentration implied a reduction of the degradation yield. In particular, the 4-NP degradation decreased from 89% at $8{\cdot}10^{-5}$ M to 84% at $3{\cdot}10^{-5}$ M, and 80% at $1{\cdot}10^{-4}$ M. According to recent studies [13, 34], high degradation yields at trace pollutant concentrations could be mainly due to the role of pollutant-catalyst surface attraction forces and the significant number of free active sites. On the other hand, the number of occupied active sites played a relevant role for degradation process at high pollutant concentrations because their saturation reduced the catalytic activity.

The effect of pH on the 4-NP degradation rates is illustrated in Figure 7. The reduction of solution pH decreased the degradation yield of 4-NP from 89% (pH 7) to 58% (pH 3) depending on the grain size. Note that pH reduction contributed to increase the attractive interactions between the pollutant molecule and the charged catalyst surface. At basic pH, these electrostatic interactions were limited due to there was a repulsion between the phenates (the molecular form of 4-NP at basic pH) and the catalyst. Figure 7 also showed that the 4-NP degradation by the catalytic oxidation process was higher than 80% at $pH \geq 7$ irrespective of the catalyst grain diameter.

Figure 8 shows a comparative of the 4-NP degradation for tested catalysts using an operating time of 4 h at pH 7. The best degradation performance was obtained with the catalysts based on HFO with a ratio of 75% Zr+25%Fe, which showed a conversion rate of 93%. Surface area of this catalyst was higher than 200 m^2/g. Overall, it can be expected that the textural parameters of heterogeneous catalysis played a relevant role for 4-NP degradation, thus contributing to increase its conversion rates.

Finally, assuming an ideal performance of tested catalyst, the following mechanism (Figure 9) has been proposed for the oxidation of 4-NP [24]:

$$H_2O_2 + \text{Catalyst (25HFe75Zr)} \longrightarrow 2OH^*, \quad (5)$$

$$2OH^* + 4 - \text{NPhOH} \longrightarrow PhO^* + H_2O + NO_2, \quad (6)$$

$$H_2O_2 + PhO^* \longrightarrow \text{intermediate products} \longrightarrow CO_2 + H_2O. \quad (7)$$

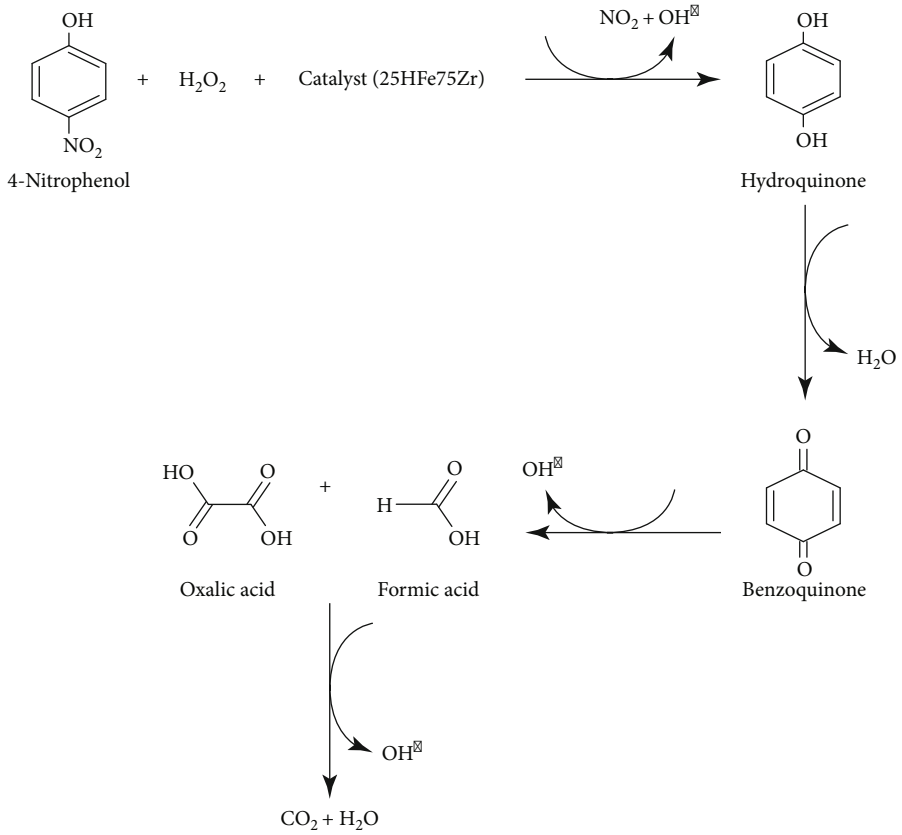

Figure 9: Illustration of degradation mechanism of 4-nitrophenol using the best catalyst obtained in this study.

Note that an adsorption interaction could occur during the oxidation according to the following equation:

$$4 - \text{NPhOH} + \text{catalyst (grains)} \longrightarrow \text{adsorption}. \quad (8)$$

Finally, it is convenient to indicate that HPLC analysis of samples obtained at different times of experiments confirmed the degradation of this pollutant where intermediate products were not found with the implemented analytical method. Therefore, further studies are required to determine if some intermediate products could be generated during this degradation process. These studies will imply the application of other analytical techniques, and their results will complement the analysis of catalyst performance in this application.

4. Conclusions

This study reports the synthesis and characterization of catalysts obtained from iron oxyhydroxide type supported on zirconium and their application in 4-NP degradation. This catalyst showed a BET surface area up to 267.66 m^2/g with the predominance of mesoporous. Textural characteristics of this type of materials contributed to enhance their efficiency for 4-NP degradation. Overall, the degradation performance of these catalysts were depended on their composition. Results showed that a 4-NP degradation efficiency up to 93% were obtained with the best catalyst (particle size of 0.4–1 mm) at pH 7, 27°C, and 4 h. This result showed that the hybrid HFO/Zr was an attractive catalytic precursor. Catalytic tests showed that the grains synthesized on the basis of HFO supported on zirconium were active in the neutral medium for 4-NP degradation. HFO-based catalysts are promising materials for the oxidation of organic compounds in water treatment.

Data Availability

Data of this paper are available on request to the corresponding author.

Conflicts of Interest

The authors declared no potential conflicts of interest with respect to the research, authorship, and/or publication of this article.

References

[1] Y. Y. Merve, S. B. Esra, and K. M. Çiğdem, "A polymer – zeolite composite for mixed metal removal from aqueous solution," *Water Science & Technology*, vol. 83, no. 5, pp. 1152–1166, 2021.

[2] H. Gaffour and M. Mokhtari, "Photocatalytic degradation of 4-nitrophenol using TiO_2 + Fe_2O_3 and TiO_2/Fe_2O_3-supported bentonite as heterogeneous catalysts," *Journal of Research Chemical Intermediates*, vol. 42, no. 6, pp. 6025–6038, 2016.

[3] S. Peretz and O. Cinteza, "Removal of some nitrophenol contaminants using alginate gel beads," *Colloids and Surfaces A: Physicochemical and Engineering Aspects*, vol. 319, no. 1-3, pp. 165–172, 2008.

[4] S. S. Sable, K. J. Shah, P. C. Chiang, and S. L. Lo, "Catalytic oxidative degradation of phenol using iron oxide promoted sulfonated-ZrO2 by advanced oxidation processes (AOPs)," *Journal of the Taiwan Institute of Chemical Engineers*, vol. 91, pp. 434–440, 2018.

[5] D. Rajkumar and K. Palanivelu, "Electrochemical degradation of cresols for wastewater treatment," *Industrial Engineering Chemistry Research*, vol. 42, no. 9, pp. 1833–1839, 2003.

[6] M. Saeed and M. Ilyas, "Oxidative removal of phenol from water catalyzed by nickel hydroxide," *Applied Catalysis B: Enviromental*, vol. 129, pp. 247–254, 2013.

[7] K. P. Mishra and P. R. Gogate, "Intensification of sonophotocatalytic degradation of p-nitrophenol at pilot scale capacity," *Ultrasonic Sonochemistry*, vol. 18, no. 3, pp. 739–744, 2011.

[8] X. Yang, J. Li, T. Wen, X. Ren, Y. Huang, and X. Wang, "Adsorption of naphthalene and its derivatives on magnetic graphene composites and the mechanism investigation," *Journal of Colloids and Surfaces A: Physicochemical and Engineering Aspects*, vol. 422, pp. 118–125, 2013.

[9] S. J. Kulkarni, R. W. Tapre, S. V. Patil, and M. B. Sawarkar, "Adsorption of phenol from wastewater in fluidized bed using coconut shell activated carbon," *Journal of Procedia Engineering*, vol. 15, pp. 300–307, 2013.

[10] S. A. Hosseini, M. Davodian, and A. R. Abbasian, "Remediation of phenol and phenolic derivatives by catalytic wet peroxide oxidation over Co-Ni layered double nanohydroxides," *Journal of the Taiwan Institute of Chemical Engineers*, vol. 75, pp. 97–104, 2017.

[11] W. Xu, J. Chen, Y. Qiu, W. Peng, N. Shi, and J. Zhou, "Highly efficient microwave catalytic oxidation degradation of 4-nitrophenol over magnetically separable $NiCO_2O_4$-$Bi_2O_2CO_3$ composite without adding oxidant," *Separation and Purification Technology*, vol. 213, pp. 426–436, 2018.

[12] M. S. A. Ángela, G. G. Gloria, and R. S. G. Nancy, "Degradation of phenol using mill scale as a Fenton-type catalyst," *Water and Environment Journal*, vol. 34, pp. 183–191, 2020.

[13] A. M. Mostafa and E. A. Mwafy, "Synthesis of ZnO/CdO thin film for catalytic degradation of 4-nitrophenol," *Journal of Molecular Structure.*, vol. 1221, p. 128872, 2020.

[14] Y. Wang, L. He, G. Lv, and X. Sun, "Experimental and theoretical insights into the RCS-involved electro-catalytic transformation of 4-nitrophenol," *Chemosphere*, vol. 262, p. 128015, 2021.

[15] M. B. Gawande, Y. Monga, R. Zboril, and R. K. Sharma, "Silica-decorated magnetic nanocomposites for catalytic applications," *Coordination Chemistry Reviews*, vol. 288, pp. 118–143, 2015.

[16] W. J. Liu, F. X. Zeng, H. Jiang, X. Zhang, and W. W. Li, "Composite Fe2O3 and ZrO2/Al2O3 photocatalyst: preparation, characterization, and studies on the photocatalytic activity and chemical stability," *Chemical. Engineering journal*, vol. 180, pp. 9–18, 2012.

[17] S. N. Basahel, T. T. Ali, M. Mokhtar, and K. Narasimharao, "Influence of crystal structure of nanosized ZrO_2 on photocatalytic degradation of methyl orange," *Nanoscale Research Letters*, vol. 10, no. 1, p. 73, 2015.

[18] D. Chen, S. Chen, Y. Jiang et al., "Heterogeneous Fenton-like catalysis of Fe-MOF derived magnetic carbon nanocomposites for degradation of 4-nitrophenol," *Royal Society of Chemistry Advances*, vol. 7, no. 77, pp. 49024–49030, 2017.

[19] N. Ayas, Y. B. Asci, and M. Yurdakul, "Using of Fe/ZrO2 catalyst to remove direct orange 26 from water by Fenton oxidation at wide pH values," *Fresenius Environmental Bulletin*, vol. 25, no. 8, pp. 3272–3279, 2016.

[20] S. S. Sable, S. C. Panchangam, and S. L. Lo, "Abatement of clofibric acid by Fenton-like process using iron oxide supported sulfonated-ZrO_2: efficient heterogeneous catalysts," *Journal of Water Process Engineering*, vol. 26, pp. 92–99, 2018.

[21] N. Lahbabi, M. Hajjaji, Z. Rais, and S. Kacim, "Oxidation of phenol on an iron-based catalyst supported on a Moroccan clay," *Africa Science*, vol. 5, no. 3, pp. 14–24, 2009.

[22] A. Espinosa de los Monteros, G. Lafaye, A. Cervantes, G. D. Angel, J. Barbier Jr., and G. Torres, "Catalytic wet air oxidation of phenol over metal catalyst (Ru,Pt) supported on TiO2–CeO2 oxides," *Catalysis Today*, vol. 258, pp. 564–569, 2015.

[23] M. Idrissi, Y. Miyah, M. Chaouch et al., "CWPO of phenol using manganese-based catalysts," *Journal of Materials Environmental Science*, vol. 5, pp. 2309–2313, 2014.

[24] I. Othman, M. Abu Haija, and F. Banat, "Catalytic properties of phosphate-coated $CuFe_2O_4$ nanoparticles for phenol degradation," *Journal of Nanomaterials*, vol. 2019, 8 pages, 2019.

[25] H. Mahmoodi, M. Fattahi, and M. Motevassel, "Graphene oxide–chitosan hydrogel for adsorptive removal of diclofenac from aqueous solution: preparation, characterization, kinetic and thermodynamic modelling," *Royal Society of Chemistry Advances*, vol. 11, no. 57, pp. 36289–36304, 2021.

[26] S. Dolatabadi, M. Fattahi, and M. Nabati, "Solid state dispersion and hydrothermal synthesis, characterization and evaluations of TiO_2/ZnO nanostructures for degradation of rhodamine B," *Desalination Water Treatment*, vol. 231, pp. 425–435, 2021.

[27] A. Garmroudi, M. Kheirollahi, S. A. Mousavi, M. Fattahi, and E. H. Mahvelati, "Effects of Graphene Oxide/TiO_2 Nanocomposite, Graphene Oxide Nanosheets and Cedr Extraction Solution on IFT Reduction and Ultimate Oil Recovery from a Carbonate Rock," in *Petroleum*, In Press, 2020.

[28] H. Asadzadeh Patehkhor, M. Fattahi, and M. Khosravi-Nikou, "Synthesis and characterization of ternary chitosan- TiO_2-ZnO over graphene for photocatalytic degradation of tetracycline from pharmaceutical wastewater," *Scientific Reports*, vol. 11, no. 1, pp. 1–17, 2021.

[29] X. Jiang, C. Peng, D. Fu et al., "Removal of arsenate by ferrihydrite via surface complexation and surface precipitation," *Applied Surface Science*, vol. 353, pp. 1087–1094, 2015.

[30] H. Wu, D. Xiaowen, D. Dayi, G. Yufeng, Z. Liguo, and H. Guangping, "Decolourization of the azo dye orange G in aqueous solution via a heterogeneous Fenton-like reaction catalysed by goethite," *Environmental Technology*, vol. 33, no. 14, pp. 1545–1552, 2012.

[31] B. Cheknane, O. Bouras, M. Baudu, J. P. Basly, and A. Cherguielaine, "Granular inorgano-organo pillared clays (GIOCs): Preparation by wet granulation, characterization and application to the removal of a Basic dye (BY28) from aqueous solutions," *Chemical Engineering Journal*, vol. 158, no. 3, pp. 528–534, 2010.

[32] V. Lenoble, O. Bouras, V. Deluchat, B. Serpaud, and J. C. Bollinger, "Arsenic adsorption onto pillared clays and iron oxides," *Journal of Colloid Interface Science*, vol. 255, no. 1, pp. 52–58, 2002.

[33] A. S. Pham, N. Shun, and E. Kohki, "Preparation of zirconium carbonate as water-tolerant solid base catalyst for glucose isomerization and one-pot synthesis of levulinic acid with solid acid catalyst," *Reaction Kinetics Mechanism Catalysis*, vol. 111, no. 1, pp. 183–197, 2014.

[34] H. Chen, Z. Sun, Z. Yang et al., "Degradation of 3,4-dichlorobenzotrifluoride by the Fenton-like process using zirconia-coated magnetite magnetic nanoparticles as an effective heterogeneous catalyst," *Environmental Science and Pollution Research*, vol. 24, no. 22, pp. 18575–18584, 2017.